BIOCHEMISTRY
including biophysical chemistry & molecular biology
Article

Biochemistry **2011,** *50,* 1347–1358 1347
DOI: 10.1021/bi101838s

Functional Epitopes for Site 1 of Human Prolactin†

Geeta Vittal Rao‡ and Charles L. Brooks*,§

‡*Ohio State Biophysics Program and* §*Departments of Veterinary Biosciences and Biochemistry, The Ohio State University, Columbus, Ohio 43210, United States*

Received November 17, 2010; Revised Manuscript Received January 11, 2011

ABSTRACT: Human prolactin (hPRL) binds two human prolactin receptor molecules, creating active heterotrimeric complexes. Receptors bind dissimilar hormone surfaces termed site 1 and site 2 in an obligate ordered process. We sought to map the functional epitopes in site 1 of hPRL. Extensive alanine mutagenesis (102 of the 199 residues) showed approximately 40% of these mutant hPRLs changed the ΔG for site 1 receptor binding. Six of these residues are within 3.5 Å of the receptor and form the site 1 functional epitopes. We identified a set of noncovalent interactions between these six residues and the receptor. We identified a second group of site 1 residues that are between 3.5 and 5 Å from the receptor where alanine mutations reduced the affinity. This second group has noncovalent interactions with other hormone residues and stabilized the topology of the functional epitopes by linking these to the body of the protein. Finally, we identified a third group of residues that are outside site 1 (> 5 Å) and extend to site 2 and whose mutation to alanine significantly weakened receptor binding at site 1 of prolactin. These three groups of residues form a contiguous structural motif between sites 1 and 2 of human prolactin and may constitute structural features that functionally couple sites 1 and 2. This work identifies the residues that form the functional epitopes for site 1 of human prolactin and also identifies a set of residues that support the concept that sites 1 and 2 are functionally coupled by an allosteric mechanism.

Human prolactin (hPRL)[1] is representative of a class of four-helix bundle hormones and cytokines (*1*, *2*). hPRL binds the hPRL receptor, creating an active trimeric complex composed of one hPRL and two receptors (*3*). The binding reaction for hPRL or any lactogenic hormone is an obligate ordered process (*4*, *5*) in which a receptor binds a surface of hPRL (site 1) inducing a conformational change in hPRL that organizes residues to form a second receptor-binding surface (site 2) capable of subsequently binding a second hPRL receptor. The hPRL receptor is composed of an extracellular domain (hPRLr), containing an N-terminal S1 subdomain and a C-terminal S2 subdomain (*6*), a single transmembrane domain, and a structurally uncharacterized intracellular domain. Studies of human lactogenic hormones suggest site 1 is composed of residues within helices 1 and 4 as well as the loop connecting helices 1 and 2 (*7*). The second receptor binds two surfaces of the heterodimeric hPRL−hPRLr complex, the first consisting of residues in helices 1 and 3 (*8*) and a receptor−receptor interface of the S2 subdomains (*9*).

Members of this class of human signaling proteins, including hPRL, growth hormone (hGH), placental lactogen (hPL), leptin, and erythropoietin, all form similar trimeric structures during receptor binding (*1*, *2*). These hormones and their interactions with receptors have been characterized by both mutagenic and structural studies. Two structures of hPRL (*10*, *11*) and a structure of mutant hPRL bound to one hPRLr have been published (*12*). In addition, several structures of mutant hPRLs or wild-type hPRL bound to the extracellular domain of the rat prolactin receptor have been published (*3*, *13*).

Energetic and structural mapping of the surfaces of hGH (*14*, *15*) and hPL (*16*) binding to the hPRLr has been reported, but the mapping of the energetics of hPRL binding to hPRLr has not been reported and compared to those of other lactogenic hormones. hPRL is the least conserved lactogenic hormone (< 25% homologous to either hGH or hPL) and may have the most unique set of binding residues. Both structural information and energetic mapping are necessary to identify residues that form noncovalent bonds with hPRLr or are required for the functional coupling of sites 1 and 2. Analysis of this information is critical for the rational design of antagonists or for understanding the mechanism by which hPRL agonists and antagonists regulate receptor activity. Site-directed mutagenesis frequently has been used to identify binding interfaces as well as interactions within prolactin that either maintain structure or functionally couple sites 1 and 2 (*4*, *17*−*35*). These studies have used a variety of functional end points to assess the effects of mutations, including binding of ^{125}I-labeled hormone to cells or membranes containing prolactin receptors or cellular biological assays that typically use growth as their end point. Mutagenic studies using these end points have not discerned binding to either site 1 or site 2 and thus failed to unambiguously identify energetically significant residues within specific binding surfaces, or in motifs that functionally couple sites 1 and 2.

In this report, we have used alanine scanning mutagenesis to evaluate 102 of the 199 residues of hPRL to determine the role of their side chains when hPRLr binds site 1. We chose the residues to be studied on the basis of data indicating their possible location

†This work was supported by a grant from the National Institutes of Health (DK072275) to C.L.B.

*To whom correspondence should be addressed: The Ohio State University, 1925 Coffey Rd., Columbus, OH 43210. Phone: (614) 292-9641. Fax: (614) 292-6473. E-mail: brooks.8@osu.edu.

[1]Abbreviations: hPRL, methionyl human prolactin; hPRLr, residues 1−210 of the extracellular domain of the methionyl hPRL receptor; $hPRLr_{211C}$, hPRLr with a C-terminal cysteinyl group; hGH, human growth hormone; hPL, human placental lactogen; IPTG, isopropyl β-D-1-thiogalactopyranoside; DTT, dithiothreitol; K_d, dissociation constant; ΔG, free energy; $\Delta\Delta G$, change in free energy; CD, circular dichroism; k_1, forward rate constant; k_{-1}, reverse rate constant; SPR, surface plasmon resonance; PDB, Protein Data Bank.

Published on Web 01/12/2011

within site 1 or 2 (the N-terminus, helices 1, 3, and 4, loop 1, and the C-terminus), residues evaluated in earlier mutagenic studies that influenced either global receptor binding or biological function (*17*−*21*), and structural studies of homologous hormone−receptor complexes (*6*, *36*). We measured the kinetics of binding of hPRLr to site 1 of the wild type and each of the alanine mutants of hPRL and calculated the kinetic rate constants, K_d values, and ΔG values to determine the effects of each of these mutations directly on site 1 binding. Differences in the ΔG values between wild-type and mutant hPRLs were calculated ($\Delta\Delta G$) and used as a measure of the effect of individual mutations. This information was used with a high-resolution (2.55 Å) hPRL−hPRLr structure (*12*) to identify the energetically important residues within site 1 and those functionally coupling site 1 with site 2.

EXPERIMENTAL PROCEDURES

Vectors, Bacterial Strains, and Mutagenesis. The pT7-7 phagemid containing the coding sequence for methionyl hPRL was prepared by Peterson et al. (*37*). The pT7-7 phagemid encoding receptor residues 1−210 and both an N-terminal methionyl and a C211-terminal cysteinyl ($hPRLr_{C211}$) was prepared by Voorhees and Brooks (*5*) from the vector provided by Sivaprasad and Brooks (*4*). We chose to couple hPRLr to the surface plasmon resonance (SPR) chip so that only site 1 binding would be evaluated in these studies. Use of the C211 residue bound to the SPR chip provided a chip surface with identical coupling chemistries. The complete sequences of each insert were confirmed by DNA sequencing (*38*). Alanine scanning mutagenesis of extensive portions of hPRL was performed by the Quikchange method (*39*). Primers for converting each of the 108 residues investigated in this study to alanine in the 199-residue hPRL were prepared and are available as Supporting Information (Appendix S1). In preliminary work, the biological activities of wild-type methionyl hPRL were similar to that of the natural hormone.

Selection of Sites of Mutation. Our goal was to investigate regions of the hPRL sequence by alanine mutagenesis that had been previously associated with hPRL receptor binding. Thus, we sought to prepare a set of mutant proteins able to bind the receptor at either site 1 or site 2. Selection of the residues for alanine mutagenesis was performed using homologous structures for hGH bound to either the extracellular domain of the hGH receptor (PDB entry 2HHR) (*40*) or hPRLr (PDB entry 1BP3) (*6*), and the structure of ovine placental lactogen bound to the rat PRLr (PDB entry 1F6F) (*36*). Hormone−receptor distances of < 3.5 Å were used to identify residues within hormone−receptor interfaces (*41*). Sequence alignments of these hormones with hPRL were subsequently used to identify sequences that might be within the receptor's binding sites. In addition, results from mutagenic studies of hPRL were used to identify additional residues (*17*−*21*). These calculations provided several sequences that were further lengthened to ensure a thorough coverage of hPRL. This method provided four long sequences, including residues P5−K42, I51−N76, A108−S135, and A167−N198, a total of 120 residues. Alanines (eight residues) and cysteines (four residues) were not investigated (leaving a total of 108 mutant hPRLs). Three residues failed to produce mutants, and three failed to express (leaving 102 mutant hPRLs). Finally, one protein failed to provide surface plasmon resonance data (leaving 101 mutant hPRLs providing essentially complete data sets). We obtained 94% coverage of the 108 mutant hPRLs we investigated. The 102 residues whose mutations to alanines were evaluated and projected on the structure of hPRL (*12*) (Figure 1, top panel). These sequences provided substantial coverage of the structural features: 7 of 14 residues of the N-terminus, 27 of 29 residues of helix 1, 19 of 34 residues of loop 1

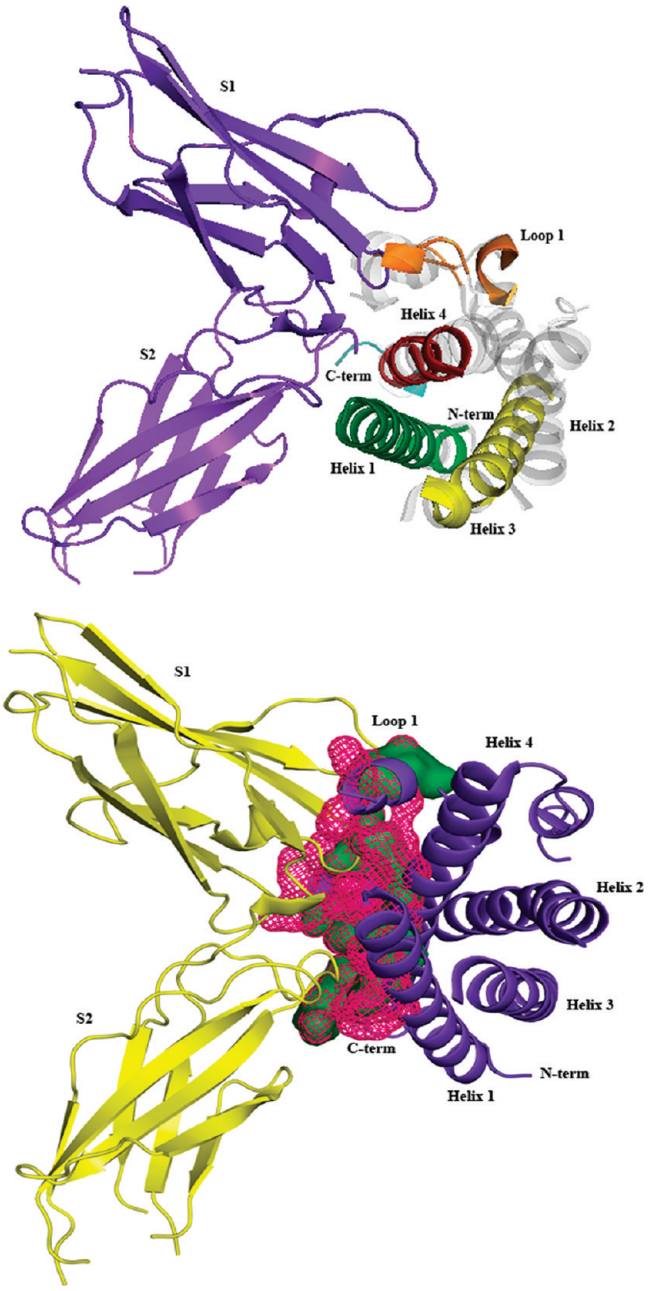

FIGURE 1: Spatial arrangement of hPRL residues studied by alanine mutagenesis. In the top panel, hPRLr is colored purple-blue and hPRL pale silver in the crystal structure of an hPRL antagonist bound to hPRLr (*12*). Superimposed colored segments in hPRL correspond to sections of the protein that were chosen for alanine scanning. These sections correspond to the following residues: N-terminus, 5−7, 10, and 12−14 (green); helix 1, 15−21 and 23−42 (green); and loop 1, 52, 53, 55−57, 59−63, 65−68, 71, and 73−76 (orange). Disruption of the C-terminal disulfide loop in PRLs has reduced the activities of these mutants: loop 2, 110; helix 3, 112−115 and 117−135 (yellow); helix 4, 168−173, 177−184, 186−190, and 192 (red); and C-terminus, 193, 194, and 196−198 (cyan). This hPRL structure has its first 11 residues truncated, a region into which four mutations were introduced in this study. In the bottom panel, hPRLr is colored yellow and hPRL purple-blue. Site 1 structural epitopes in hPRL (27 residues 5 Å from hPRLr) are colored red. Colored green are the 14 residues within site 1 that display significant $\Delta\Delta G$ values.

(mostly in the C-terminal end), 1 of 7 residues connecting helices 2 and 3, 23 of 27 residues of helix 3, 21 of 33 residues in helix 4, and 4 of 6 residues in the C-terminus. Helix 2 and loop 2 were not investigated.

Expression, Folding, and Purification of Proteins. Wild-type hPRL, $hPRLr_{C211}$, and the 102 alanine hPRL mutants were expressed and purified as previously described (*4*, *37*). Briefly, each of the plasmids was transformed into BL21(DE3) *Escherichia coli* and selected by resistance to ampicillin. Single colonies were selected and expanded by continuous log-phase growth at 37 °C to an A_{600} of 0.3. Expression was initiated by addition of IPTG to a concentration of 0.4 mM. Expression was continued for 3−4 h, and the bacteria were homogenized by two passes through a French pressure cell. Inclusion bodies were collected by centrifugation, solubilized in 100 mM Tris (pH 11) and 4.5 M urea, and folded during dialysis into 20 mM Tris (pH 7.5). Folding was followed by application to a DEAE-Sephadex column and elution with a NaCl gradient. Each protein was dialyzed against 10 mM NH_3HCO_3 and subsequently lyophilized under conditions with a 60−100 °C temperature differential and a vacuum of less than 100 μbar (*42*). Final yields (dry weight) for each liter of bacterial fermentation were generally between 2 and 30 mg of protein. These procedures have been shown to produce wild-type hPRLs with activities indistinguishable from those of pituitary isolates.

Characterization of Recombinant Proteins. The recombinant proteins were evaluated for size and purity using SDS-containing 12% PAGE under reducing conditions. Protein folding was assessed by fluorescence (model LS-55, Perkin/Elmer) (*43*) and circular dichroism (CD) spectroscopy (model 202, Aviv) (*44*) at 20 °C in 10 mM Tris (pH 8.2) and 150 mM NaCl. We chose these two methods to identify grossly unfolded proteins on the basis of the environment of the intrinsic tryptophan fluorochromes and the extent of helix formation.

Preparation of $hPRLr_{C211}$ for Disulfide Bonding to a SPR Chip. $hPRLr_{C211}$, containing a cysteine at position 211, was suspended in 10 mM sodium phosphate buffer (pH 7.4). $hPRLr_{C211}$ was treated with an equimolar amount of DTT for 5 min at room temperature to reduce the free cysteine at the C-terminus of the protein. $hPRLr_{C211}$ was desalted with a PD-10 column (Amersham Biosciences), concentrated to 500 μL using a Microcon YM-10 centrifugal concentrator (Millipore), and stored at 4 °C. $hPRLr_{C211}$ concentrations were determined by measuring the absorbance at 280 nm and using a calculated extinction coefficient of 66140 cm^{-1} M^{-1} (*45*).

Thiol Coupling to the CM5 Chip. Experiments were performed using a Biacore 3000 (GE Healthcare) at 25 °C. $hPRLr_{C211}$ was thiol-coupled to the carboxymethylated dextran surface of a CM5 sensor chip using the engineered C-terminal cysteine. The flow rate during ligand coupling was 5 μL/min. The chip surface was prepared by being washed with HBS-EP buffer [10 mM HEPES (pH 7.4), 150 mM NaCl, 3 mM EDTA, and 0.005% (v/v) Tween 20 (Biacore, Piscataway, NJ)], followed by activating each flow cell with 10 μL of 50 mM *N*-hydroxysuccinimide (NHS) and 20 mM *N*-ethyl-*N*′-(dimethylaminopropyl)-carbodiimide (EDC). Disulfide groups were introduced via injection of 20 μL of 80 mM 2-(2-pyridinyldithio)ethaneamine in 50 mM $NaHCO_3$ (pH 8.5). To ensure that ligand only bound via thiol coupling, the remaining NHS/EDC groups were blocked using 35 μL of 1 M ethanolamine (pH 8.5). $hPRLr_{C211}$ at a concentration of 25−35 μg/mL was diluted 10-fold in 10 mM sodium acetate buffer (pH 4.5). To prevent protein degradation at low pH, 5−8 μL of this dilute protein was immediately injected over the activated chip surface. $hPRLr_{C211}$ at a concentration of 2.5−3.0 μg/mL was linked through a thiol−disulfide exchange, fixing approximately 100 RU to the chip surface. The unreacted groups on the chip were blocked using 35 μL of 50 mM cysteine in 20 mM sodium acetate (pH 4.5) and 1 M NaCl. A control lane was prepared on each chip by activating and blocking the chip surface as described above, with no protein bound.

Binding of hPRLs to hPRLr. Before the receptor binding experiments with the hPRL mutants were performed, the activity of the hPRLr was assessed by flowing 1 μM wild-type hPRL over the chip surface for 4 min. Dissociation was monitored for 8 min, after which the chip surface was regenerated with 10 μL of 4.0 M $MgCl_2$ (pH 7.4) to remove bound hormone. Evaluation of the kinetic binding data yielded an affinity constant that was similar to previously published data (*16*) that had been produced using SPR technology and human proteins. Therefore, we concluded that both hPRLr and hPRL were well-folded and that the immobilization of $hPRLr_{C211}$ did not influence hPRL binding.

All binding experiments were performed in HBS-EP buffer at a flow rate of 50 μL/min. Concentrations of hPRL mutants chosen for kinetic experiments were 0, 10, 100, 1000, and 5000 nM. These concentrations of each mutant hPRL were injected in random order over the chip surface, and the hPRL−hPRLr binding was recorded for 4 min followed by an 8 min HBS-EP buffer injection recorded to follow hPRL dissociation. The kinetic data were used to calculate the on and off rate constants and, subsequently, the K_d and ΔG for each hPRL. The chip surface was regenerated by being treated with 10 μL of 4 M $MgCl_2$ (pH 7.4). Five minutes after regeneration, a buffer injection was performed to clean the needle of $MgCl_2$ to minimize carryover into subsequent protein injections. Binding data were doubly referenced prior to evaluation to ensure that the affinity constant was reliable and accurate (*46*). Groups of 4−10 mutant hPRLs were assessed in separate, sequential runs; approximately 1 week of continuous SPR operation was required to collect the entire data set. Injections of 1 μM wild-type hPRL were performed at the beginnings and ends of each run to evaluate changes of the $hPRLr_{C211}$ associated with the chip surface. In all, there were 16 pairs of wild-type hPRL controls run during the evaluation of all 102 mutant hPRLs. The data for mutagenesis, expression and purification, purity, circular dichroism and fluorescence spectra, raw SPR data, forward and reverse rate constants, and dissociation constants for these 102 hPRL mutants are available (Supporting Information, Appendix S1).

Evaluation of the Kinetic Data. BIAevaluation 3.0 (Biacore) was used to simultaneously fit three to five binding curves for each mutant to a simple 1:1 Langmuir binding model. This model was chosen for fitting the data because avidity effects are highly unlikely at the low surface density of immobilized $hPRLr_{C211}$ (< 100 RU), and we have previously demonstrated that chip protein densities and pump rates used in our studies did not produce such methodological bias (*4*, *5*). The association and dissociation rate constants (k_1 and k_{-1}, respectively) were calculated, and from these data, the dissociation constants ($K_d = k_{-1}/k_1$) and free energies [$\Delta G = -RT \ln(1/K_d)$] were calculated.

No systematic changes in the control reactions of wild-type hPRL binding to the hPRLr were observed during the binding analysis of the 102 mutant hPRLs. No differences in the K_d values of the controls run at the beginning and end of each analytical run were detected by paired-T analysis. In addition, no changes in the K_d values of the controls were observed when analyzed by one-way analysis of variance.

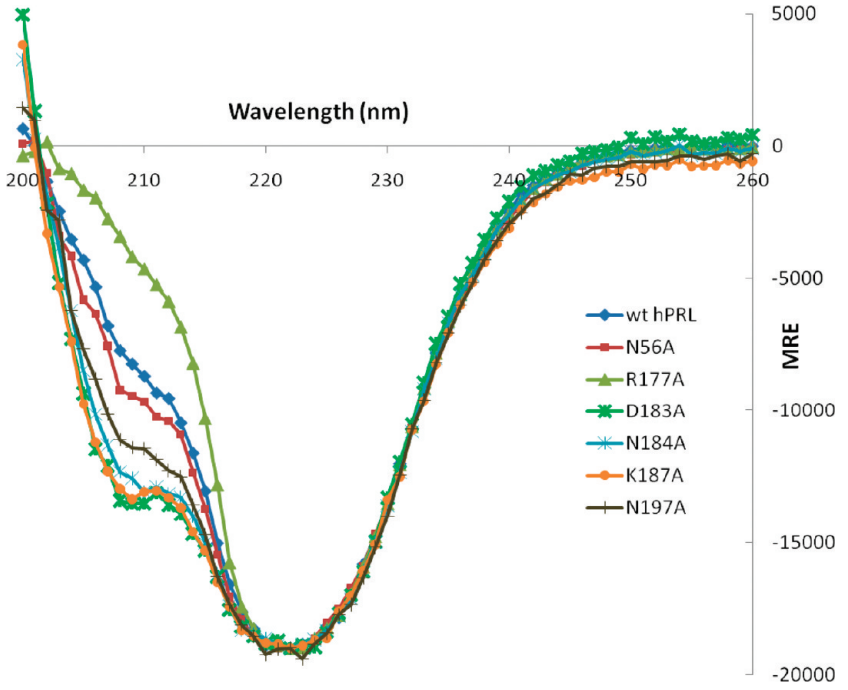

FIGURE 2: CD spectra of wild-type and six mutant hPRLs with significant $\Delta\Delta G$ values for site 1 and noncovalent contacts with hPRLr. An α-helix has a characteristic CD spectrum with a negative peak at 222 nm because of the n$-\pi^*$ electron orbital transition and one at 208 nm because of the $\pi-\pi^*$ electron orbital transition. The mean residue elipticity (MRE) is expressed in units of degrees square centimeters per residue per millimole (*44*). The CD spectra for wild-type hPRL and mutants were measured, and the 222 nm peak for each of the mutants was normalized to that of the wild type for comparison of differences in the 208 nm peak between the wild type and a mutant. Normalization was conducted because many mutants had a CD signal weaker than that of the wild type. This is most likely due to differences in concentration between proteins, although slight differences in helical content cannot be ruled out. The protein concentrations were calculated by measuring the absorbance at 280 nm and using a calculated extinction coefficient (*45*).

Identification of the Structural Epitopes in Site 1 of hPRL. Identification of the residues that constitute site 1 is necessary for describing the structural epitopes, of which functional epitopes are a subset. The structure of a mutant hPRL (Δ1−11, Q12S, G129R) bound in a 1:1 complex with hPRLr (*12*) was used to identify residues constituting site 1 of hPRL because this structure had the highest resolution (2.55 Å) at the time of analysis. A 5 Å distance between hPRL and hPRLr was used as the cutoff to identify site 1 structural epitopes using PyMol (*47*).

Identification of Functional Epitopes in Site 1 of hPRL. We chose to define functional epitopes as residues revealing a high probability of forming noncovalent contacts with hPRLr. hPRL residues lying within 3.5 Å of hPRLr were identified using PyMol. We chose a cutoff distance of 3.5 Å to identify noncovalent interactions using COOT (*48*).

RESULTS

Characterization of Recombinant Proteins. Wild-type and mutant hPRLs were >95% pure with a molecular mass of 23 kDa as judged by SDS-containing 12% PAGE. $hPRLr_{C211}$ was a single protein with a molecular mass of 24 kDa (Supporting Information, Figure S1 and Appendix S1). Fluorescence spectroscopy characterized the tryptophan environment (W91 and W150), while CD spectroscopy characterized the secondary structure. Generally, neither was changed by mutation. The close overlay of the fluorescence spectra of wild-type and six alanine mutant hPRLs located in site 1 and displaying significant $\Delta\Delta G$ indicates the structures have not been changed significantly by alanine mutation (Supporting Information, Figure S2). The CD spectra for these six mutant hPRLs were similar to that of wild-type hPRL, displaying a minimum at 222 nm but often a small shoulder at 208 nm (Figure 2). The hormones were all α-helical as judged by their CD spectra. Five mutant hPRLs, including Q12A, F19A, L127A, R177A, and D178A, displayed significant changes in their CD spectra, suggesting these residues are critical to the native structure of the hormone. Each of these structurally disrupted mutants displayed a significant reduction in the strength of hPRLr binding. As expected from the available structural information (*3*, *6*, *12*), the $hPRLr_{C211}$ spectra indicated a β-sheet structure.

Surface Plasmon Resonance Data and Calculation of Rate Constants, Dissociation Constants, ΔG Values, and $\Delta\Delta G$ Values. Kinetic SPR data describing binding and dissociation were successfully obtained from 101 mutant hPRLs; one hPRL mutant, H195A, failed to provide sufficient data for analysis. In addition, 32 single-concentration control experiments were performed with wild-type hPRL at the beginning and end at each group of mutant hormones (Supporting Information, Table S1). Because of the cost and time involved in such a large study, each mutant hPRL concentration was run only once in the SPR studies. The forward rate constants for the mutant hPRLs binding to $hPRLr_{C211}$ varied approximately 10000-fold (between 5×10^2 and 4.2×10^6 M^{-1} s^{-1}), with most of the k_1 values indicating a slower forward rate compared to the mean k_1 for wild-type hPRL (3.67×10^5 M^{-1} s^{-1}). The k_{-1} values varied over a more narrow 30-fold range (from 2.3×10^{-2} to 7.3×10^{-4} s^{-1}). These values described a more rapid dissociation for most of the mutant hPRLs compared to the mean k_{-1} obtained for wild-type hPRL (2.0×10^{-3} s^{-1}). The k_{-1}/k_1 ratios were used to determine the dissociation constants (K_d) for mutant hPRLs. The K_d values for the mutant hPRLs varied over a 10000-fold range (between 0.71 and 7690 nM). The dissociation constants were used to calculate the free energy (ΔG) for all wild-type and mutant hPRLs [$\Delta G = -RT \ln(1/K_d)$]. The K_d values

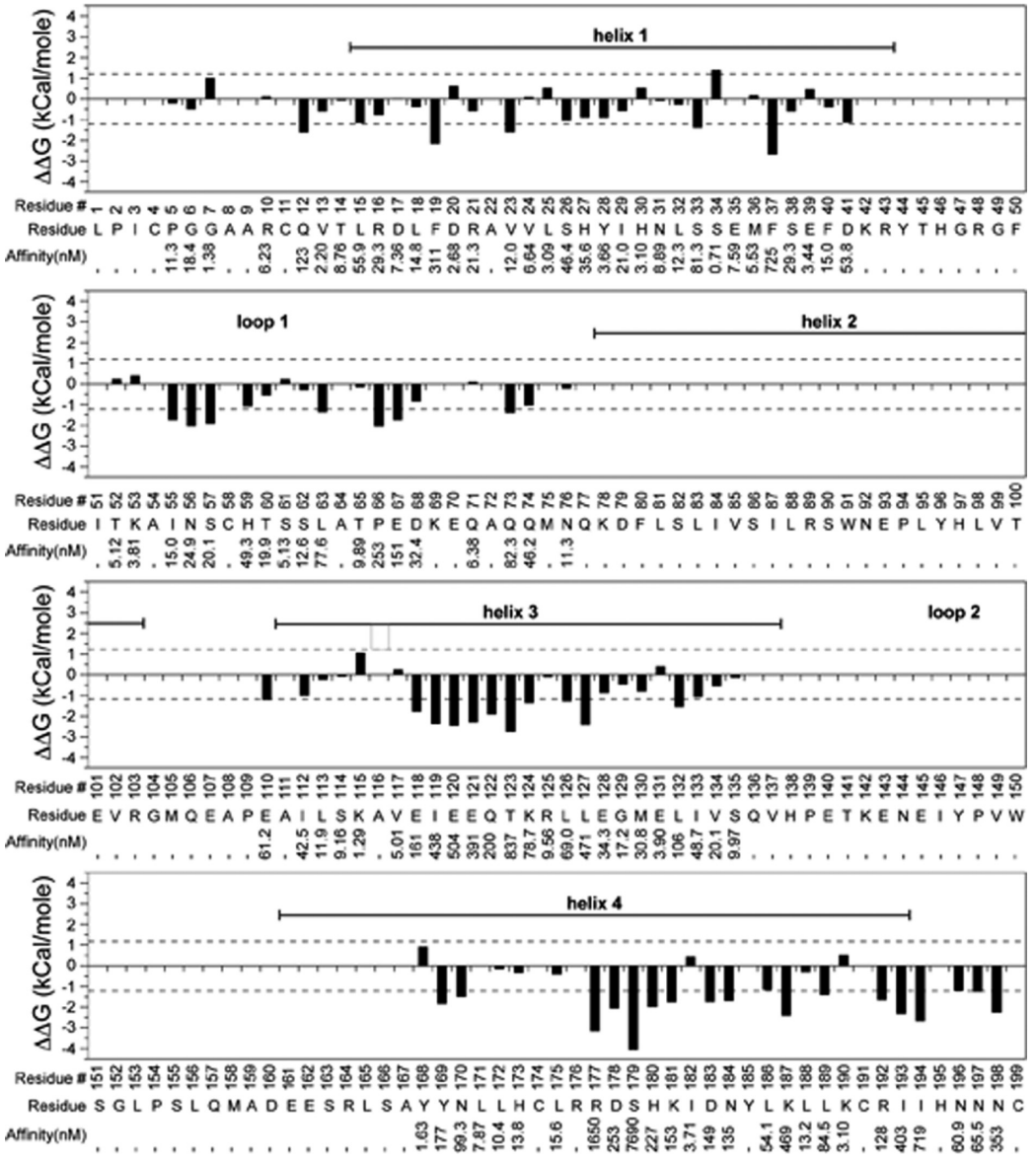

FIGURE 3: Summary of the locations and effects of alanine mutations on the K_d and $\Delta\Delta G$ of hPRL. The K_d and ΔG for wild-type hPRL are 7.47 nM and −11.09 kcal/mol, respectively.

for wild-type and mutant hPRLs were used to calculate the change in free energy ($\Delta\Delta G$) associated with alanine mutations $\{\Delta\Delta G = -RT \ln[K_{d(mutant)}/K_{d(wild\text{-}type)}]\}$. This calculation will produce negative values for $\Delta\Delta G$ when the mutation weakens the binding of hPRL to hPRLr at site 1. K_d, k_1, k_{-1}, ΔG, and $\Delta\Delta G$ values for each mutant hPRL are provided in Table S2 of the Supporting Information. The mean K_d for wild-type hPRL was 7.47 nM, similar to values previously obtained by SPR techniques (*4*, *5*, *16*). The average free energy for wild-type hPRL was calculated to be −11.09 kcal/mol with a standard deviation of 0.40 kcal/mol (3.6% coefficient of variation).

The $\Delta\Delta G$ values for the alanine mutations of hPRLs varied between −4.07 and 1.41 kcal/mol. The distribution of these $\Delta\Delta G$ values is shown in Figure S3 of the Supporting Information. To identify mutations that significantly altered the free energy of binding hPRLr, we selected mutant hPRLs for which the absolute values of $\Delta\Delta G$ values were greater than 3 times the standard deviation ($3 \times 0.40 = 1.20$ kcal/mol) of the ΔG for wild-type hPRL ($\Delta G = -11.09$ kcal/mol). One mutant hPRL (S34A) bound with a significantly increased strength (0.71 nM), while 40 mutant hPRLs exhibited significantly weaker binding (60.9−7690 nM) (Figure 3 and Table S2 of the Supporting Information).

Identification of Functional Epitopes. Forty-one residues displayed significant $\Delta\Delta G$ values when mutated to alanine. Of the 41 residues with significant $\Delta\Delta G$ values, nine are within 3.5 Å of the hPRLr surface (Figure 1, bottom panel, and Table 1), and five residues are within 3.5−5.0 Å of hPRLr. The mutant hPRLs within site 1 (< 5.0 Å) displaying significant $\Delta\Delta G$ values include I55, N56, P66, E67, Q73, R177, H180, K181, D183, N184, K187, K192, N197, and N198. These site 1 residues are located in loop 1 (five residues), helix 4 (six residues), and the adjacent C-terminus (three residues). Thirteen of the 14 hPRL residues in the site 1 structural interface have identifiable noncovalent interactions with residues within hPRL, hPRLr, or both. Table 2 shows nine residues are within 3.5 Å of hPRLr. Six of these nine residues (N56 in loop 1, R177, D183, N184, and K187 in helix 4, and N197 in the C-terminus) were identified as functional epitopes because they displayed significant $\Delta\Delta G$ values and revealed contacts compatible with noncovalent interactions with surface residues of hPRLr (Table 2 and Figure 4, top panel). Four of these six

Table 1: Residues of hPRL within the Site 1 Interface

27 hPRL residues within 5.0 Å of hPRLr	18 hPRL residues within 3.5 Å of hPRLr	14 hPRL residues with significant $\Delta\Delta G$ values within 5.0 Å of hPRLr	9 hPRL residues with significant $\Delta\Delta G$ values within 3.5 Å of hPRLr
H27		NS[a]	
H30	H30	not significant	
N31	N31	not significant	
I51		NS[a]	
T52	T52	not significant	
I55		I55[b]	
N56	N56	N56[c]	N56[c]
P66		P66[b]	
E67	E67	E67	E67
D68	D68	not significant	
K69	K69	NS[a]	
E70		NS[a]	
Q73		Q73[b]	
H173	H173	not significant	
R176	R176	NS[a]	
R177	R177	R177[c]	R177[c]
H180	H180	H180[b]	H180[b]
K181		K181[b]	
D183	D183	D183[d]	D183[d]
N184	N184	N184[d]	N184[d]
Y185		NS[a]	
K187	K187	K187[d]	K187[d]
L188	L188	not significant	
C191	C191	NS[a]	
R192		R192[b]	
N197	N197	N197[d]	N197[d]
N198	N198	N198[b]	N198[b]

[a]Not studied. [b]Detectable noncovalent bonds to other hPRL residues. [c]Detectable noncovalent bonds to hPRLr residues. [d]Detectable noncovalent bonds to both hPRL and hPRLr residues.

functional residues also have noncovalent interactions within hPRL. One residue, E67, provided a significant $\Delta\Delta G$ and was within 3.5 Å of hPRLr but displayed no identifiable noncovalent contacts with either hPRLr or hPRL. Residues H180 and N198 are within 3.5 Å of hPRLr but have noncovalent interactions with only other residues in the hormone (Table 2).

On the basis of earlier mutagenesis studies, helices 1 and 4 as well as loop 1 were thought to contain residues that constitute site 1 (*20*, *24*). Surprisingly, we found no functional epitopes in helix 1. This is because all helix 1 residues that significantly affect binding to hPRLr at site 1 are >5 Å from the hPRLr and nonionic (F19, V23, S33, S34, and F37).

In addition to the 14 residues found within the hPRL−hPRLr interface, 88 residues that were outside this interface were tested (>5.0 Å from hPRLr). Of these 88 residues, 27 have significant $\Delta\Delta G$ values. Mutation of one residue to alanine (S34A, 0.78 nM and $\Delta\Delta G$ of 1.41 kcal/mol) produced an approximately 10-fold increase in the strength of hPRLr binding. Mutation of the 26 remaining residues to alanine reduced the strength of binding of hPRLr at site 1 ($\Delta\Delta G$ between -1.21 and -4.07 kcal/mol).

For site 2, six hPRL residues were identified to be within 3.5 Å of the rat PRLr (PDB entry 3EW3) (Table 3 and Figure S4 of the Supporting Information). Although an approximation, these hPRL residues include D17, R21, R125, E128, G129, and L132 of hPRL and are found in eithe helix 1 or 3. P2 and Y3 are not further considered because they represent an N-terminal sequence spliced from ovine placental lactogen to hPRL. Each of these residues was tested, but only the L132A mutation displayed a significant $\Delta\Delta G$ for site 1 binding. The influence of these residues in receptor binding at site 2 remains to be determined. When these residues were evaluated for noncovalent interactions with rat PRLr bound at site 2 of hPRL, with the exception of G129 each of the residues displayed several interactions with atoms in rat PRLr, hPRL, or both (Table S3 of the Supporting Information).

Finally, five mutant hPRLs exhibited significant changes in their CD spectra: Q12A, F19A, L127A, R177A, and D178A. These residues are likely critical for the maintenance of the hormone's structure. Three of the mutant hPRLs are >5 Å from site 1 or 2 (F19A, L127A, and D178A). The Q12A mutation is within 5 Å of site 2 but has no noncovalent interactions. Only the R177A mutant is within 3.5 Å of hPRLr in site 1 and is predicted to have noncovalent interactions with hPRLr (Figure 2). The CD spectrum for R177A hPRL has a reduced signal at 208 nm when compared to that of wild-type hPRL or those of the other five mutants (Figure 2).

DISCUSSION

Analysis of the Mutagenic Studies. We sought to provide a high degree of sequence coverage by alanine mutagenesis to allow identification of functional epitopes in site 1 of hPRL. Of the 108 residues we desired to test, we succeeded in obtaining data for 101 residues, providing coverage of 94%. These residues composed the N-terminus, helices 1, 3, and 4, loop 1, and the C-terminus; we did not perform mutagenesis in either helix 2 or loop 2 (Figure 1, top panel). To ensure that the immobilized ligand was equally active and functional during the multiday collection of SPR data, we bound wild-type hPRL to $hPRLr_{C211}$ at the beginning and end of each batch of mutant hPRLs. No changes in wild-type hPRL binding were detected between the K_d values obtained from the beginning and end of each set of samples when analyzed by a paired T analysis. A change in the K_d values over the course

Table 2: Site 1 hPRL Residues with a Significant $\Delta\Delta G$ Binding to hPRL and hPRLr[a]

functional epitope of hPRL	$\Delta\Delta G$ (kcal/mol)	interaction with hPRL residues	interaction with hPRLr residues
Asn56	−2.06	none	Asn56 OD1−N Gly44 Asn56 OD1−Cβ Glu43
Glu67	−1.75	none	none
Arg177[b]	−3.16	none	Arg177 Nε−O HOH228 Arg177 Nε−O Trp72 Arg177 Cδ−O Trp72 Arg177 Cζ−O Trp72 Arg177 Cζ−Oε2 Glu43 Arg177 NH1−Oε2 Glu43 Arg177 NH1−O Trp72 Arg177 NH2−Oε2 Glu43 Arg177 NH2−Oδ2 Asp96 Arg177 NH2−Oγ1 Thr74
His180	−1.93	His180 Nε2−O HOH208 His180 Cβ−O Arg176 His180 Cβ−O Arg177	none
Asp183	−1.75	Asp183 Cβ−O Ser179 Asp183 Cβ−O HOH208 Asp183 Cγ−O HOH208 Asp183 Cγ−Nζ Lys187 Asp183 Oδ2−O HOH208 Asp183 Oδ2−NZ Lys187 Asp183 Oδ1−N His27 Asp183 Oδ1−Oγ Ser26 Asp183 Oγ1−Nζ Lys187 Asp183 Oδ−Cε1 Lys187 Asp183 Oδ1−Cδ Lys187	Asp183 Oδ2−Nε2 His188
Asn184	−1.70	Asn184 Cβ−O HOH208 Asn184 Cβ−O His180	Asn184 Oδ1−Nζ Lys17 Asn184 Cγ−Nζ Lys17 Asn184 Nδ2−O Trp139
Lys187	−2.43	Lys187 Cδ−Oδ1 Asp183 Lys187 Cε−Oδ1 Asp183 Lys187 Nζ−Oδ1 Asp183 Lys187 Nζ−Oδ2 Asp183 Lys187 Nζ−Cγ Asp183 Lys187 Nζ−Cβ His27 Lys187 Nζ−Nδ1 His27	Lys187 Cδ−O HOH224
Asn197	−1.27	Asn197 Nδ2−Cα Arg192	Asn197 Nδ2−O HOH230
Asn198	−2.25	Asn198 Nδ2−O His195 Asn198 Nδ2−O Asn196	none

[a] $\sum\Delta\Delta G$ for residues with hPRLr contacts: $-2.06 + -3.16 + -1.75 + -1.70 + -2.43 + -1.27 = -12.37$ kcal/mol. These interface residues were not studied: K69, R176, and C191. These interface residues were studied but had no significant $\Delta\Delta G$ values: H30, N31, T52, D68, H173, and L188. Note that only the Cβ atom and beyond of each hPRL residue was used for identifying interactions. Interactions with the hPRL backbone were not taken into consideration for this analysis. [b] Altered CD spectrum.

of the SPR experiment could not be detected when assessed by one-way analysis of variance. These analyses indicate that the $hPRLr_{C211}$ linked to the chip surface had not degraded during the course of data collection. These controls provide confidence that the SPR binding studies for the mutant hPRLs are valid and that our analytical system did not significantly change over the course of data collection.

The K_d values for all wild-type hPRL binding controls were used to calculate the mean (K_d = 7.47 nM). The mean ΔG for wild-type hPRL was -11.09 ± 0.40 kcal/mol, with a coefficient of variation of 3.6%. We concluded that the measurement of rate constants for our mutant proteins could be performed with sufficient precision to allow accurate calculations of $\Delta\Delta G$ values and identification of functional epitopes. We chose to define a significant change in ΔG as 3 times the standard deviation of the wild-type hPRL value (1.20 kcal/mol), providing a low probability of identifying residues that do not affect site 1 receptor binding. Comparisons of the changes in the free energy between wild-type and mutant hPRLs ($\Delta\Delta G$) identified 41 of the 101 alanine mutations where the binding was changed (Figure 5). If we had chosen to use two standard deviations as our cutoff, 16 additional mutant hPRLs would be identified. Fifty-seven proteins displayed $\Delta\Delta G$ values that were within ±2 standard deviations of that of wild-type hPRL (Table S3 of the Supporting Information). These data describe a bimodal distribution (Figure S3 of the Supporting Information). The distribution of $\Delta\Delta G$ values indicates that the single-alanine mutations produced a group of proteins that did not bind hPRLr like wild-type hPRL. When mutants influenced site 1 binding, they overwhelmingly bound more weakly to $hPRLr_{C211}$. This observation suggests that many of the wild-type residues are preferential, and their presence creates a nanomolar affinity that provides a functional binding isotherm within the physiological range of hPRL concentrations observed in humans. Residues identified by this method displayed fluorescence and circular dichroism spectra largely similar to those of wild-type hPRL, suggesting that in most cases single-alanine mutations did not significantly disrupt protein folding. Thus, this set of mutant hPRLs identifies residues whose side

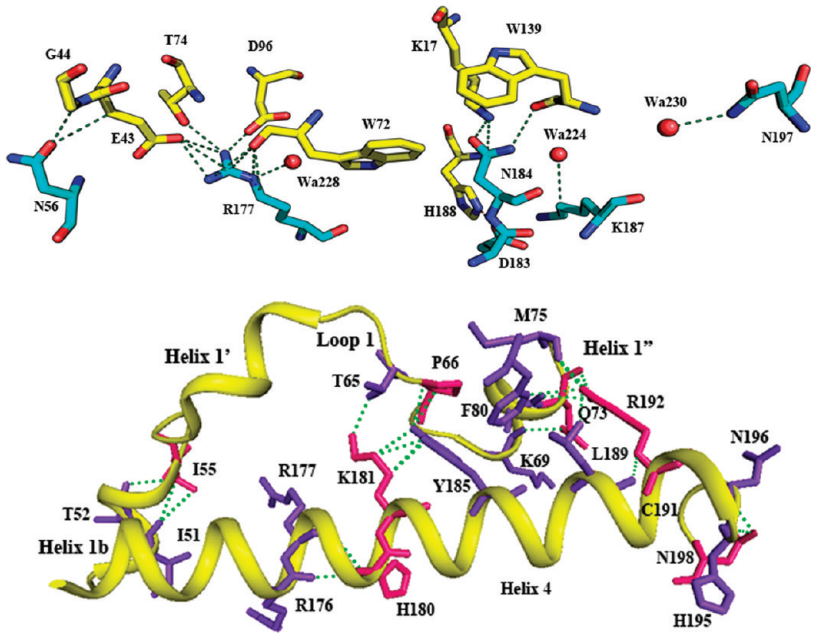

FIGURE 4: Noncovalent bonds between hPRL and hPRLr in site 1 receptor-binding epitopes. In the top panel, residues are color-coded according to atom type, with the carbon atoms of hPRL colored cyan and those of hPRLr yellow. Bonds are shown as dashed lines. There are three water molecules in the site 1 interface that have important noncovalent interactions with hPRL residues. In the bottom panel, site 1 residues that significantly impact binding affinity are colored pink, while the hPRL partners with which they interact are colored purple-blue. Noncovalent interactions between hPRL residues are shown as green dashed lines.

Table 3: Site 2 Structural Epitopes of hPRL

location in hPRL		structural epitopes within 5.0 Å of rat PRLr at site 2	structural epitopes within 3.5 Å of rat PRLr at site 2	residues within 5.0 Å of site 2 of rat PRLr with a significant $\Delta\Delta G$ value for site 1
N-terminus	P1[a]	NS[c]		
	P2	NS[c]	P2	Q12[b]
	Y3[a]	NS[c]	Y3[a]	
	P8[a]	NS[c]		
	G9[a]	NS[c]		
	K10[a]	NS[c]		
	C11	NS[c]		
	Q12[b]	significant		
	I13	not significant		
helix 1	D17	not significant	D17	
	L18	not significant	R21	
	R21	not significant		
	A22	NS[c]		
	L25	not significant		
	Y28	not significant		
helix 3	Q122	significant		Q122
	R125	not significant	R125	L126
	L126	significant	E128	L132
	E128	not significant	G129	
	G129	not significant	L132	
	L132	significant		

[a]Not present in wild-type hPRL. [b]Altered CD spectrum. [c]Not studied.

chains are likely to be functionally significant and reside in site 1 or form a motif required for the site 1 binding-induced conformation change of hPRL that functionally couples sites 1 and 2.

The residues identified with significant $\Delta\Delta G$ values can be placed into the three groups that we believe are required to couple sites 1 and 2. These include site 1 residues that directly interact with the receptor (Table 2), site 2 residues that directly interact with the receptor (Table 3), and residues that provide interactions necessary for functional coupling of sites 1 and 2. Further, some residues may participate in both receptor binding and functional coupling of sites 1 and 2. These relationships are consistent with our previous biophysical studies (*4*, *5*) that demonstrate an obligate ordered binding scheme that requires a functional coupling between sites 1 and 2 and a structural motif coupling the two receptor binding sites.

Analysis of Site 1 Mutations with Respect to Site 1 Binding. We used the 2.55 Å structure of N-truncated G129R hPRL of Svensson et al. (PDB entry 3D48) (*12*) so we could most

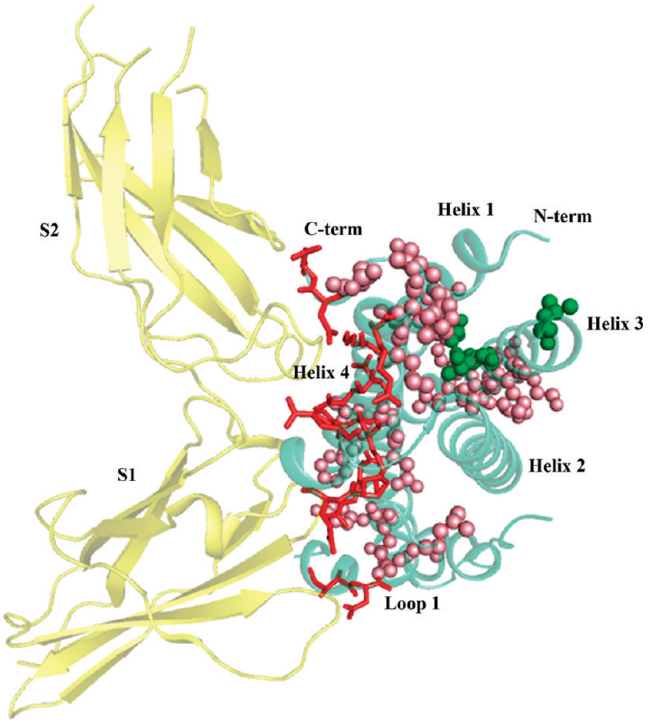

FIGURE 5: Summary of residues that when mutated to alanine had significant $\Delta\Delta G$ values. hPRLr and the hPRL antagonist to which it is bound (*12*) are colored gold and green-cyan, respectively. Red sticks and green and pink spheres together represent 41 hPRL residues found to significantly impact the binding affinity for hPRLr ECD at site 1. Red sticks correspond to 14 residues within 5.0 Å of hPRLr at site 1. These are I55, N56, P66, E67, Q73, R177, H180, K181, D183, N184, K187, R192, N197, and N198. Residues colored green are in site 2 and within 5.0 Å of the rat PRLr (*3*); they include Q12, Q122, L126, and L132. Pink spheres represent 23 residues that are not in site 1 or site 2 (> 5.0 Å from hPRLr). These are F19, V23, S33, S34, F37, S57, L63, E110, E118, I119, E120, E121, T123, K124, L127, Y169, N170, D178, S179, L189, I193, I194, and N196.

accurately identify residues within either 5.0 or 3.5 Å of any hPRLr atom in site 1 (Table 1). Examination of the structural details revealed that two residues (N56 and R177) displayed noncovalent interactions only with the hPRLr, two residues (H180 and N198) displayed noncovalent interactions only within hPRL, and four residues displayed noncovalent interactions between hPRLr and within hPRL (D183, N184, K187, and N197). Finally, one residue (E67) displayed a significant $\Delta\Delta G$ ($\Delta\Delta G = -1.75$ kcal/mol) and was within 3.5 Å of hPRLr, but no noncovalent interactions were identified with either hPRL or hPRLr. E67 is located on the surface of the heteromolecular structure and is 3.99 Å from a fixed water. Perhaps E67 participates in a long-range electrostatic interaction that is removed by mutation to alanine. We have not evaluated electrostatic contributions in our analysis.

Noncovalent bonding in the interface of site 1 shows significant coupling between the hPRLr and surface residues of hPRL as well as between the surface and more interior residues of hPRL (Table 2 and Figure 4, top and bottom panels). H180, D183, N184, and K187 share noncovalent interactions with other residues contained in helix 4; these occur primarily within three or four residues (one turn) of this helix. These interactions stabilize helix 4. Residues N197 and N198 in the C-terminal disulfide loop interact with other loop residues, including R192, H195, and N196 (Table 2 and Figure 4, bottom panel). The disulfide loop is defined by C191 and C199 that are held in a stable position because C191 is a C-terminal member of helix 4. These structures fix the disulfide loop to the C-terminus of helix 4 and reduce the level of movement of this disulfide loop. This is in contrast to the N-terminal disulfide loop in which the NMR-derived structure of Teilum et al. (*11*) suggests greater freedom of movement. Disruption of the C-terminal loop by alanine replacements of N197 and N198 weakens site 1 binding by elimination of noncovalent interactions within the C-terminal loop of hPRL and with hPRLr. Disruption of the C-terminal disulfide loop in PRLs reduces the biological activities of these mutants (*49*, *50*).

Several interactions occur between residues within and between helices 1 and 4. D183 and K187 each form noncovalent interactions with H27. A disulfide bond between C58 (loop 1) and C174 (helix 4) also restricts the relative movements of elements in the N-terminal portion of the protein and helix 4. Despite the spatial articulation of these hPRL elements, no interactions were observed between any residues of helix 1 and hPRLr. Previous mutagenic studies (*24*) of residues in helix 1 indicated a disruption of global binding. When we restrict the effects of mutations to binding site 1, a different picture emerges in which several alanines in helix 1 display significant $\Delta\Delta G$ values (−2.18 kcal/mol for F19, −1.62 kcal/mol for V23, −1.39 kcal/mol for S33, 1.41 kcal/mol for S34, and −2.68 kcal/mol for F37) but are too distant from the hPRLr to form noncovalent interactions. Seven to ten mutations identified by global binding (*24*) described insignificant changes in $\Delta\Delta G$ for site 1. Three residues (V23, S34, and F37) had both changes in global binding affinity and significant changes in $\Delta\Delta G$ for site 1. These observations indicate that identification of the functional epitopes for receptor binding requires that both functional and structural information be employed. Four of the five helix 1 residues (F19, S33, S34, and F37) with significant $\Delta\Delta G$ values form noncovalent interactions with helix 4 and within helix 1 mostly between residues in an $N \pm 3$ and $N \pm 4$ relationship. These interactions will stabilize helix 1 and create a stable structural relationship between the two helices involved in site 1 binding. We were unable to identify noncovalent bonds for V23, but it is located in a hydrophobic pocket and may be necessary for an optimal steric relationship.

The site 1 structural epitopes were largely either polar or ionic with only one residue considered nonpolar (I55). Functional epitopes (Figure 4) were either asparagines (N56, N184, and N197) or charged (R177, D183, and K187). If site 1 functional epitopes are completely identified, then the sum of free energy changes caused by mutating these residues should approach the free energy of the wild-type hormone binding hPRLr-ECD only if there is no functional coupling present. These six residues comprising the functional epitopes provided a $\sum\Delta\Delta G$ of −12.34 kcal/mol, an energy similar to the free energy of hormone−receptor binding. We have evaluated the ΔG values derived from short-range noncovalent bonds. Thus, we anticipate that ionic interactions between the nonhydrated interfaces would also provide additional binding energy. Finally, alanine mutations do not allow evaluation of short-term noncovalent bonds that utilize the backbone atoms (*51*); residues with such bonds would not be identified by alanine mutagenesis.

Mutation of D183 causes a 20-fold reduction in the strength of hPRLr binding and has an important polar interaction with H188 of hPRLr (Figure 4, top panel). Recently, H188 of hPRLr has been shown to be an important determinant for site 1 binding (*52*). Similarly, N184, which has polar interactions with the side chain and backbone of K17 and W139 of hPRLr, reduces the strength of

Table 4: Comparison of the Site 1 Residues of hGH, hPL, and hPRL That Contribute to hPRLr Binding

hPRL[a]				hGH[a,b]			hPL[a,b]		
protein or mutant	K_d (nM)	$\Delta\Delta G$ (kcal/mol)	*n*-fold change in K_d	protein or mutant	K_d (nM)	*n*-fold change in K_d	protein or mutant	K_d (nM)	*n*-fold change in K_d
wild type	7.47	0.0	1.0	wild type	0.033	1.0	wild type	0.6	1.0
H27A	35.6	NS[c]	4.7	H18A[d]	4.50	136	H18A[d]	not det[e]	–
H30A	3.10	NS[c]	0.4	H21A[d]	0.30	9.1	H21A[d]	17	28
S34A	0.71	1.41	0.1	F25A	0.23	7.0	I25A	9.2	15
N56A	249	−2.05	33.3	S51A	–	–	S51A	5.9	10
L63A	77.6	−1.36	10.4	I58A	0.61	18.5	I58A	20	33
K69A	–	–	–	R64A	–	–	M64A	8.0	13
E70A	–	–	–	E65A	–	–	E65A	8.5	14
E67A	151	−1.76	20.2	S62A	0.36	10.9	S62A	18	30
D68A	32.4	NS[c]	4.4	N63A	0.14	4.2	N63A	33	55
H173A	13.8	NS[c]	1.8	Y164A	–	–	Y164A	17	28
R176A	–	–	–	R167A	25.0	758	R167A	90	150
R177A	1650	−3.16	221	K168A	0.61	18.5	K168A	67	112
H180A	227	−2.00	50.8	D171A	0.037	1.1	D171A	15	25
K181A	153	−1.76	20.5	K172A	7.20	218	K172A	not det[e]	–
D183A	149	−1.74	19.9	E174A[d]	12.0	364	E174A[d]	not det[e]	–
N184A	135	−1.69	18.1	T175A	0.076	2.3	T175A	29	48
Y185A	–	–	–	F176A	0.83	25.2	F176A	100	167
K187A	469	−2.42	62.8	R178A	0.23	7.0	R178A	38	63

[a]Measurements of hPRL−hPRLr and hPL−hPRLr affinities were performed by kinetic SPR studies, while hGH−hPRLr affinities were determined by equilibrium competition studies. [b]Data for hGH were from ref *59*; data for hPL were from ref *16*. [c]Not significant. [d]H18, H21, and E174 constitute a Zn^{2+} binding site required for a high-affinity interaction of hGH or hPL with hPRLr. [e]Not detectable binding.

binding by 18-fold. Mutation of N184 has been shown to reduce biological activity by up to 50% (*24*). K187 and N197 have interactions with hPRLr through fixed water molecules (Figure 4, top panel). R177 contributes to the free energy of site 1 binding, which has been noted in mutagenic (*19*, *25*) and structural (*12*) studies. Mutation of R177 to alanine causes a 221-fold decrease in the strength of hPRLr binding, the largest value observed for any of the residues in site 1. Indeed, the R177 side chain atoms are involved in a tight hydrogen bonding and ion pairing network with hPRLr residues E43, T74, D96, and W72 and water. The long carbon backbone of R177 has hydrophobic contacts with hPRLr W72 (Figure 4, top panel), but in our study, the R177A mutant displays an altered CD spectrum, indicating a change in the hormone's structure and providing ambiguity in the interpretation.

Effects of Site 2 Mutations on Site 1 Binding. Six of the 102 residues that we studied may be within site 2 (< 3.5 Å from rat PRLr in PDB entry 3EW3). The identity of site 2 in hPRL is problematic because one must use the heterologous structure of a mutant hPRL bound to two extracellular domains of rat PRLr (*3*). We identified D17 and R21 in helix 1, R125, E128, G129, and L132 in helix 3, and two residues in the N-terminus as possible site 2 structural epitopes (Figure S4 of the Supporting Information). The N-terminal residues are not further considered because they represent the N-terminal sequence of ovine placental lactogen spliced to hPRL. Of these six residues, only L132 displayed a significant $\Delta\Delta G$ for site 1 binding. Whether any or all of these six residues would provide significant $\Delta\Delta G$ for site 2 binding remains to be determined. Three additional residues, Q12, Q122, and L126, are found between 3.5 and 5.0 Å from rat PRLr, and each of these residues displays a significant $\Delta\Delta G$ when replaced with alanine. These residues may be required to maintain a functional chemical topology at site 2 as well as being functionally linked to site 1.

Analysis of Binding at Site 1 with Mutations External to Site 1 or 2. Overall, the presence of these covalent and noncovalent interactions between structural elements provides a picture of how hPRL−hPRLr binding could initiate and propagate a conformational change from site 1 to site 2. Mapping the 41 residues with significant $\Delta\Delta G$ values onto the structure of Svensson et al. (*12*) shows a contiguous motif extending from the interface of site 1 to residues within 3.5 Å of site 2 (Figure 5). Twenty-three of the residues external to sites 1 and 2 displayed significant $\Delta\Delta G$ values when mutated to alanine and tested for site 1 binding. Functional reciprocity (*53*−*55*) within the thermodynamically linked residues of this motif is required for a functionally linked conformational change induced by hPRLr binding at site 1. We and others have provided evidence of hPRL-induced conformational changes (*3*−*5*). Thus, alanine mutations that are distal to site 1 and included in the motif required for conformation changes may influence site 1 binding. The evidence necessary to strengthen this argument will be to determine the effects of these mutations on site 2 binding when site 1 is bound by hPRLr and by double-mutation studies (*55*). We anticipate that mutation of the residues in the motif identified in this work would also influence site 2 binding and that the residues whose mutation failed to influence site 1 binding would for the most part not influence binding of hPRLr at site 2.

Potential for the Development of hPRL Receptor Antagonists. Mutant hPRLs with a stronger affinity for site 1 but an impaired affinity for site 2 are candidate antagonists. The G129R mutation allows hPRL to bind hPRLr at site 1 but not site 2 for steric reasons (*56*). We have found that S34A hPRL binds hPRLr at site 1 1 order of magnitude more strongly than wild-type hPRL. Three additional mutations of hPRL, including G7A, K115A, and Y168A, also increase the strength of site 1 binding between 4.7- and 6-fold, although these mutations did not change the ΔG significantly. Exploration of combinations of these structural changes may provide superior hPRLr antagonists. The hPRL mutant S179D has been shown to be an effective growth antagonist (*57*), and S179A in our study produced the maximal decrease in site 1 affinity when mutated to alanine (Figure 2). The loss of site 1 affinity in our study supports the observation of Walker and colleagues, who observed a significant

reduction in the ED_{50} required to stimulate the growth of Nb2 cells by S179A hPRL (*58*). S179 is located in helix 4 but is not located within 5.0 Å of hPRL. Thus, S179 may be a critical residue in a motif coupling sites 1 and 2 and may influence hPRLr binding at site 2.

Comparison of Site 1 Functional Epitopes of hGH, hPL, and hPRL Binding hPRLr. Structural and mutagenic information for hGH, hPL, and now hPRL binding to hPRLr is available. Cunningham and Wells (*59*) mutated 44 hGH residues to alanine and determined their abilities to compete with [^{125}I]hGH for hPRL receptor binding. This approach identified 12 residues whose mutation to alanine significantly reduced the affinity for the hPRL receptor (Table 4) and were noted to all be located in hGH's binding interface for the hPRL receptor (*15*). Alanine mutants of hPL and their abilities to bind site 1 of hPRLr by SPR methods also have been recently reported (*16*). The methods used to identify functional epitopes in hGH were significantly different from those used in hPRL or hPL. The relative changes in binding strength for specific residues were not correlated. hGH, hPL, and hPRL sequences were compared by using the alignment proposed by Nicoll et al. (*60*). Our data and those of either Cunningham and Wells (*59*) or Walsh and Kossiakoff (*16*) reveal that sequences in loop 1 and helix 4 contain residues that bind the hPRL receptor. Comparison of the sequences within helix 4 that correspond to functional epitopes in hPRL, hPL, and hGH does not reveal deletions or additions; this suggests a similar spatial presentation of the functional residues within these helices. Comparison of the residues identified in hGH, hPL, and hPRL reveals a substantial, but not complete, overlap of the sets of functional epitopes (Table 4). These are consistent with the argument that binding interfaces are plastic (*61*) and somewhat dissimilar collections of interface residues can be bound effectively by hPRLr.

Finally, each of these lactogenic hormones binds Zn^{2+}. Zn^{2+} increases the site 1 affinity of hGH and hPL for hPRLr, but Zn^{2+} reduces the strength of binding of hPRL to hPRLr (*5*). When H18, H21, and E174, residues involved in Zn^{2+} binding of hGH, are mutated to alanine, the binding of hPRLr to site 1 was significantly weakened. In hPRL, residues H27, H30, and D183 are involved in Zn^{2+} binding. Mutation of H27 or H30 to alanine does not influence hPRLr binding at site 1 in the absence of Zn^{2+}. Mutation of D183 to alanine weakened the K_d of hPRLr binding by 19.9-fold in the absence of Zn^{2+}.

ACKNOWLEDGMENT

We thank Jeff Voorhees, Scott Walsh, Eric Roush, Cynthia Shuman, and Samuel Jayakanthan for helpful discussions. We are grateful to Jon Vang for assisting in the data collection and processing and to Ian Kleckner for help with PyMol. Thanks to Mike Zianni and his staff at the PMGF facility for their efficient sequencing of mutant DNAs. We also thank Gordon Renkes at the Analytical Chemistry facility for help with CD studies.

SUPPORTING INFORMATION AVAILABLE

Materials supporting these studies. This material is available free of charge via the Internet at http://pubs.acs.org.

REFERENCES

1. Mott, H. R., and Campbell, I. D. (1995) Four-helix bundle growth factors and their receptors: Protein-protein interactions. *Curr. Biol. 5*, 114–121.
2. Chaiken, I. M., and Williams, W. V. (1996) Identifying structure-function relationships in four-helix bundle cytokines: Toward *de novo* mimetics design. *Trends Biotechnol. 14*, 369–375.
3. Broutin, I., Jomain, J. B., Tallet, E., van Agthoven, J., Raynal, B., Hoos, S., Kragelund, B. B., Kelly, P. A., Ducruix, A., England, P., and Goffin, V. (2010) Crystal structure of an affinity-matured prolactin complexed to its dimerized receptor reveals the topology of hormone binding site 2. *J. Biol. Chem. 285*, 8422–8433.
4. Sivaprasad, U., and Brooks, C. L. (2004) Mechanism of ordered lactogen receptor binding by human prolactin. *Biochemistry 43*, 13755–13765.
5. Voorhees, J., and Brooks, C. L. (2010) Obligate ordered binding of human lactogenic cytokines. *J. Biol. Chem. 285*, 20022–20030.
6. Somers, W., Ultsch, M., De Vos, A. M., and Kossiakoff, A. A. (1994) The X-ray structure of a growth hormone-prolactin receptor complex. *Nature 372*, 478–481.
7. Kossiakoff, A. A. (2004) The structural basis for biological signaling, regulation, and specificity in the growth hormone-prolactin system of the hormones and receptors. *Adv. Protein Chem. 68*, 147–169.
8. Bole-Feysot, C., Goffin, V., Edery, M., Binart, N., and Kelly, P. A. (1998) Prolactin (PRL) and its receptor: Actions, signal transduction pathways, and phenotypes observed in PRL receptor knockout mice. *Endocr. Rev. 19*, 225–268.
9. Van Agthoven, J., England, P., Goffin, V., and Broutin, I. (2010) Structural Characterization of the Stem-Stem Dimerization Interface between Prolactin Receptor Chains Complexed with the Natural Hormone. *J. Mol. Biol. 404*, 112–126.
10. Keeler, C., Dannies, P. S., and Hodsdon, M. E. (2003) The tertiary structure and molecular dynamics of human prolactin. *J. Mol. Biol. 328*, 1105–1121.
11. Teilum, K., Hoch, J. C., Goffin, V., Kinet, S., Martial, J. A., and Kragelund, B. B. (2005) Solution structure of human prolactin. *J. Mol. Biol. 351*, 810–823.
12. Svensson, L. A., Bondensgaard, K., Norskov-Lauritsen, L., Christensen, L., Becker, P., Andersen, M. D., Maltesen, M. J., Rand, K. D., and Breinholt, J. (2008) Crystal structure of a prolactin receptor antagonist bound to the extracellular domain of the prolactin receptor. *J. Biol. Chem. 283*, 19085–19094.
13. Jomain, J. B., Tallet, E., Broutin, I., Hoos, S., van Agthoven, J., Ducruix, A., Kelly, P. A., Kragelund, B. B., England, P., and Goffin, V. (2007) Structural and thermodynamic bases for the unique properties of del 1−9-G129R-hPRL, a pure prolactin receptor antagonist. *J. Biol. Chem. 282*, 33118–33131.
14. Duda, K. M., and Brooks, C. L. (2003) Identification of residues outside the two binding sites that are critical for activation of the lactogenic activity of human growth hormone. *J. Biol. Chem. 278*, 22734–22739.
15. Somers, W., Ultsch, M., De Vos, A. M., and Kossiakoff, A. A. (1994) The X-ray structure of human growth hormone-prolactin receptor complex. *Nature 372*, 478–481.
16. Walsh, S. T. R., and Kossiakoff, A. A. (2006) Crystal Structure and Site 1 Binding Energetics of Human Placental Lactogen. *J. Mol. Biol. 358*, 773–784.
17. Luck, D. N., Gout, P. W., Beer, C. T., and Smith, M. (1989) Bioactive recombinant methionyl bovine prolactin: Structure-function studies using site-specific mutagenesis. *Mol. Endocrinol. 3*, 822–831.
18. Luck, D. N., Gout, P. W., Kelsay, K., Atkinson, T., Beer, C. T., and Smith, M. (1990) Recombinant methionyl bovine prolactin: Loss of bioactivity after single amino acid deletions from putative helical regions. *Mol. Endocrinol. 4*, 1011–1016.
19. Luck, D. N., Huyer, M., Gout, P. W., Beer, C. T., and Smith, M. (1991) Single amino acid substitutions in recombinant bovine prolactin that markedly reduce its mitogenic activity in Nb2 cell cultures. *Mol. Endocrinol. 5*, 1880–1886.
20. Goffin, V., Norman, M., and Martial, J. A. (1992) Alanine-scanning mutagenesis of human prolactin: Importance of the 58−74 region for bioactivity. *Mol. Endocrinol. 6*, 1381–1392.
21. Goffin, V., Struman, I., Mainfroid, V., Kinet, S., and Martial, J. A. (1994) Evidence for a second receptor binding site on human prolactin. *J. Biol. Chem. 269*, 32598–32606.
22. Maruyama, O., Kato, T., Wakabayashi, K., and Kato, Y. (1994) Amino acids in the amino terminal region of the rat prolactin contribution to PRL-receptor binding and Nb2 cell proliferation activity. *Biochem. Biophys. Res. Commun. 205*, 312–319.
23. Maciejewski, P. M., Peterson, F. C., Anderson, P. J., and Brooks, C. L. (1995) Mutation of serine 90 to glutamic acid mimics phosphorylation of bovine prolactin. *J. Biol. Chem. 270*, 27661–27665.
24. Kinet, S., Goffin, V., Mainfroid, V., and Martial, J. A. (1996) Characterization of lactogen receptor-binding site 1 of human prolactin. *J. Biol. Chem. 271*, 14353–14360.

25. Kato, Y., Maruyama, O., Chung, H.-E., Tomizawa, K., and Kato, T. (1996) Amino acids in highly conserved regions near the C-terminus of rat prolactin (PRL) play critical roles similar to those in binding of human GH to the PRL receptor. *Biochem. Biophys. Res. Commun. 222*, 547–552.
26. Ho, C., Kato, T. K., Wakabayashi, K., and Kato, Y. (1996) Increased thermo-stability of rat prolactin after replacing glutamic acid at position 118 by lysine. *Zool. Sci. 13*, 915–919.
27. Kato, Y., Tomizawa, K., and Kato, T. (1997) Enhancement of the receptor binding and Nb2 proliferation activities of rat prolactin by site-directed mutagenesis. *Zool. Sci. 14*, 147–152.
28. Gertler, A. (1997) Recombinant analogues of prolactin, growth hormone, and placental lactogen: Correlations between physical structure, binding characteristics, and activities. *J. Mammary Gland Biol. Neopl. 2*, 69–80.
29. Sun, Z., Li, P. S., Dannies, P. S., and Lee, J. C. (1996) Properties of human prolactin (PRL) and H27A-PRL, a mutant that does not bind Zn. *Mol. Endocrinol. 10*, 265–271.
30. Sun, Z., Lee, M. S., Rhee, H. K., Arrandale, J. M., and Dannies, P. S. (1997) Inefficient secretion of human H27A-prolactin, a mutant that does not bind Zn^{2+}. *Mol. Endocrinol. 11*, 1544–1551.
31. Peterson, F. C., and Brooks, C. L. (2004) Different elements of mini-helix 1 are required for human growth hormone or prolactin action via the prolactin receptor. *Protein Eng., Des. Sel. 17*, 417–424.
32. Keeler, C., Jablonski, E. M., Albert, Y. B., Taylor, B. D., Myszka, D. G., Clevenger, C. V., and Hodsdon, M. E. (2007) The kinetics of binding human prolactin, but not growth hormone, to the prolactin receptor vary over a physiologic pH range. *Biochemistry 46*, 2398–2410.
33. Tettamanzi, M. C., Keeler, C., Meshack, S., and Hodsdon, M. E. (2008) Analysis of site-specific histidine protonation in human prolactin. *Biochemistry 47*, 8638–8647.
34. Keeler, C., Tettamanzi, M. C., Meshack, S., and Hodsdon, M. E. (2009) Contribution of individual histidines to the global stability of human prolactin. *Protein Sci. 18*, 909–920.
35. DePalatis, L., Almgren, C. M., Patmastan, J., Troyer, M., Woodrich, T., and Brooks, C. L. (2009) Structure and function of a new class of human prolactin antagonists. *Protein Expression Purif. 66*, 121–130.
36. Elkins, P. A., Christinger, H. W., Sandowski, Y., Sakal, E., Gertler, A., de Vos, A. M., and Kossiakoff, A. A. (2000) Ternary complex between placental lactogen and the extracellular domain of the prolactin receptor. *Nat. Struct. Biol. 7*, 808–815.
37. Peterson, F. C., Anderson, P. J., Berliner, L. J., and Brooks, C. L. (1999) Expression, folding, and characterization of small proteins with increasing disulfide complexity by a pT7-7-derived phagemid. *Protein Expression Purif. 15*, 16–23.
38. Sanger, F., Nicklen, S., and Coulson, A. R. (1977) DNA sequencing with chain-terminating inhibitors. *Proc. Natl. Acad. Sci. U.S.A. 74*, 5463–5467.
39. Wang, W., and Malcolm, B. A. (1999) Two-stage PCR protocol allowing introduction of multiple mutations, deletions and insertions using QuikChange™ site-directed mutagenesis. *BioTechniques 26*, 680–682.
40. de Vos, A. M., Ultsch, M., and Kossiakoff, A. A. (1992) Human growth hormone and extracellular domain of its receptor: Crystal structure of the complex. *Science 255*, 306–312.
41. Humphrey, W., Dalke, A., and Schulten, K. (1996) VMD: Visual molecular dynamics. *J. Mol. Graphics 14*, 33–38.
42. Matejtschuk, P. (2007) Lyophilization of Proteins. In Methods of Molecular Biology (Day, J. G., and Stacey, G. N,, Eds.) Vol. 368, Chapter 4, pp 59−72, Humana Press, Totowa, NJ.
43. Lakowicz, J. R. (2006) Principles of Fluorescence Spectroscopy, 3rd ed., Springer, New York.
44. Greenfield, N. J. (2006) Using circular dichroism spectra to estimate protein secondary structure. *Nat. Protoc. 1*, 2876–2890.
45. Pace, C. N., Vajdos, F., Fee, L., Grimsley, G., and Gray, T. (1995) How to measure and predict the molar absorption coefficient of a protein. *Protein Sci. 4*, 2411–2423.
46. Rich, R. L., and Myszka, D. G. (2000) Advances in surface plasmon resonance biosensor analysis. *Curr. Opin. Biotechnol. 11*, 54–61.
47. DeLano, W. L. (2002) The PyMOL molecular graphics system, DeLano Scientific, San Carlos, CA.
48. Emsley, P., and Cowtan, K. (2004) Coot: Model building tools for molecular graphics. *Acta Crystallogr. D60*, 2126–2132.
49. Doneen, B. A., Bewley, T. A., and Li, C. H. (1979) Studies on prolactin. Selective reduction of disulfide bonds of ovine hormone. *Biochemistry 18*, 4851–4860.
50. Necessary, P. C., Andersen, T. T., and Ebner, K. E. (1985) Activity of alkylated prolactin and human growth hormone in receptor and cell assays. *Mol. Cell. Endocrinol. 39*, 247–254.
51. Wagner, C. R., and Benkovic, S. J. (1990) Site-directed mutagenesis: A tool for enzyme mechanism dissection. *Trends Biotechnol. 8*, 263–270.
52. Kulkarni, M. V., Tettamanzi, M. C., Murphy, J. W., Keeler, C., Myszka, D. G., Chayen, N. E., Lolis, E. J., and Hodsdon, M. E. (2010) Two independent histidines, one in human prolactin and one in its receptor, are critical for pH-dependent receptor recognition and activation. *J. Biol. Chem. 285*, 38524–38533.
53. Wymann, J. (1948) Heme proteins. *Adv. Protein Chem. 4*, 407–531.
54. Wymann, J., and Gill, S. J. (1990) Binding and Linkage, University Science Books, Mill Valley, CA.
55. DiCera, E. (1998) Site-specific analysis of mutational effects in proteins. *Adv. Protein Chem. 51*, 59–119.
56. Chen, W. Y., Ramamoorthy, P., Chen, N., Sticca, R., and Wagner, T. E. (1999) A human prolactin antagonist, hPRL-G129R, inhibits breast cancer cell proliferation through induction of apoptosis. *Clin. Cancer Res. 5*, 3583–3593.
57. Chen, T.-J., Kuo, C. B., Tsai, K. F., Liu, J.-W., Chen, D.-Y., and Walker, A. M. (1985) Development of recombinant human prolactin receptor antagonists by molecular mimicry of the phosphorylated hormone. *Endocrinology 139*, 606–616.
58. Walker, A. M. (2006) Therapeutic potential of S179D prolactin—From prostate cancer to angioproliferative disorders: The first selective prolactin receptor modulator. *Expert Opin. Invest. Drugs 15*, 1257–1267.
59. Cunningham, B. C., and Wells, J. A. (1991) Rational design of receptor-specific variants of human growth hormone. *Proc. Natl. Acad. Sci. U.S.A. 88*, 3407–3411.
60. Nicoll, C. S., Mayer, G. L., and Russell, S. M. (1986) Structural features of prolactins and growth hormones that can be related to their biological properties. *Endocr. Rev. 7*, 169–203.
61. Atwell, S., Ultsch, M. H., De Vos, A. M., and Wells, J. A. (1997) Structural plasticity in a remodeled protein-protein interface. *Science 278*, 1125–1128.